Volume Graphics (2006)
T. Möller, R. Machiraju, T. Ertl, M. Chen (Editors)

Multi-Dimensional Transfer Function Design Using Sorted Histograms

Claes Lundström[†], Patric Ljung[‡], and Anders Ynnerman[‡]

[†]Center for Medical Image science and Visualization (CMIV), Linköping University, and Sectra-Imtec AB
[‡]Division for Visual Information Technology and Applications, Linköping University

Abstract

Multi-dimensional Transfer Functions (MDTFs) are increasingly used in volume rendering to produce high quality visualizations of complex data sets. A major factor limiting the use of MDTFs is that the available design tools have not been simple enough to reach wide usage outside of the research context, for instance in clinical medical imaging. In this paper we address this problem by defining an MDTF design concept based on improved histogram display and interaction in an exploratory process. To this end we propose sorted histograms*, 2D histograms that retain the intuitive appearance of a traditional 1D histogram while conveying a second attribute. We deploy the histograms in medical visualizations using data attributes capturing domain knowledge e.g. in terms of homogeneity and typical surrounding of tissues. The resulting renderings demonstrate that the proposed concept supports a vast number of visualization possibilities based on multi-dimensional attribute data.*

Categories and Subject Descriptors (according to ACM CCS): I.3.3 [Computer Graphics]: Picture/Image Generation – Viewing algorithms; I.3.6 [Computer Graphics]: Methodology and Techniques – Interaction techniques; I.3.7 [Computer Graphics]: Three-Dimensional Graphics and Realism – Color, shading, shadowing, and texture;

1. Introduction

Visualization applications are often faced with great challenges in form of advanced user objectives and complex data sets. A good example is medical imaging where the diagnostic assessments require precise information while the data sets are problematic; they may have uncalibrated scale, noisy features or overlapping tissue value ranges. Moreover, a clear trend is that multi-variate data sets are becoming more common, such as dual source volumes from the coming generation of Computed Tomography (CT) modalities.

An approach that has been employed to achieve these advanced visualizations is Direct Volume Rendering (DVR) using Multi-Dimensional Transfer Functions (MDTFs). Even though MDTFs have been successfully applied in some cases, there are prohibitive drawbacks in other situations. First of all, the complexity of the design tools is a major obstacle for wide-spread acceptance in non-research environments. For instance, the requirements from the medical imaging field are extremely demanding: the time available to achieve the visualization is merely a few minutes while the diagnostic question requires far from trivial Transfer Functions (TFs). A second drawback is that there are still many visualization tasks that cannot be achieved by the previously proposed methods.

The concepts of this paper are based on our experience of clinical DVR usage. A first insight is that the largest potential to both enhance visualization quality and simplify user interaction lies in fully exploiting the user's domain knowledge of the data set and the task at hand. Furthermore, there are clear disadvantages with fully automatic methods, e.g. static TF presets. When exploring the data set by changing and refining the visualization, more information can be obtained.

The first part of our design concept for MDTFs is the *sorted histogram*, consisting of a traditional 1D histogram where the data values are sorted and colored according to a second attribute. Figure 1 shows an initial example. Com-

† clalu@cmiv.liu.se
‡ {plg,andyn}@itn.liu.se

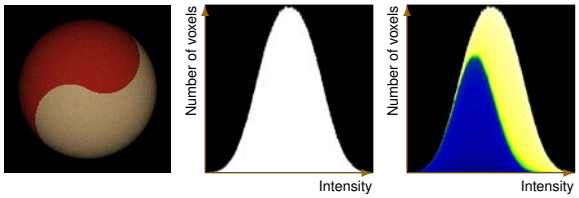

Figure 1: *Benefit of sorted histograms. Left: This synthetic data set consists of two parts with overlapping Gaussian distributions. Middle: An ordinary histogram does not reveal that there are two objects. Right: A sorted histogram, color-mapped to a classifying attribute, can reveal the underlying structure: 'yin' maps to blue (dark) and 'yang' to yellow (light).*

pared to other 2D histograms, the occurrence of intensity values is always readily visible, enabling an at-a-glance overview of this most important dimension. (In the histogram context we use "1D" and "2D" to describe the number of attributes that are shown in the histogram.) Selecting a region in a sorted histogram is then a straightforward way of creating a 2D TF. A useful variant is the *relative sorted histogram* that displays the relative distribution of second attribute values for each intensity value.

The second component of our concept is a set of classifying attributes, where we employ several attributes that effectively capture domain knowledge, as complements to the common gradient-based measures. These attributes include range weight and local variance, and we show that they enable additional visualization possibilities within an MDTF.

Finally, we present a TF design process making use of the above contributions. Employing an exploratory paradigm we let the user dynamically define attributes, display them in sorted histograms, select regions in the histogram that defines classification criteria, and iterate this procedure. The resulting MDTF is continuously refined based on the conclusions made in the process. A main advantage of this approach is that any type of classifying information can be incorporated in a uniform way.

2. Related work

This section will briefly review related research on MDTF design. Two-dimensional TFs were initially proposed by Levoy [Lev88] in 1988, suggesting that gradient magnitude is a valuable additional attribute apart from the intensity value. Kindlmann and Durkin [KD98] proposed a TF model by adding the first and second derivative along the gradient direction as extra attributes. This 3D histogram yields good separation of material boundaries and enables a more advanced rendering. Kniss et al. [KKH02] extended this model with TF design widgets. Another boundary enhancement is the 2D lighting TF by Lum and Ma [LM04]. For each sample in the rendering process, a second sample is taken at an offset determined by the gradient. In recent work Šereda et al. [ŠVSG06] propose the *LH-histogram* to overcome some limitations of intensity vs. gradient histograms. The two attributes are the low and high extremes around each voxel after applying a gradient based boundary model. Furthermore, curvature-based TFs have been shown to add visualization possibilities [HKG00, KWTM03], e.g. separation within isosurfaces.

A drawback of MDTFs is the high complexity that make them too cumbersome for most usage outside the research context. One way to simplify the TF construction is to avoid specification in the data domain and let the user implicitly define the TF through more intuitive types of interaction. One example is iterative selection in a gallery of automatically generated TF variations [HHKP96, MAB*97, KG01]. Further examples include high-dimensional TFs created through data probing [TLM03] and interaction with a clustering algorithm [TM04b]. Moreover, efficient tissue classification has been achieved through creation of additional attributes based on straight-forward user knowledge of the data set [LLY05].

Explicit design of MDTFs guided by 2D histograms is employed in some of the above approaches. A typical implementation displays intensity and gradient axes, where the occurrence is color-coded [KKH02]. The LH-histogram [ŠVSG06] has a similar 2D display. In 2D histograms the variations in occurrence are not intuitive to perceive compared to 1D histograms, where the occurrence maps to height. Recently, Lundström et al. [LYL*06] introduced the α-histogram that further increases the usefulness of 1D-histograms by amplifying spatially coherent value ranges.

Several types of attributes have been proposed for additional TF dimensions. Gradients and second derivatives are common [KKH02], and other boundary measures exist [ŠVSG06]. These approaches are less suitable for more noisy data such as Magnetic Resonance (MR) images [PBSK00] and they do not capture interior characteristics of materials. These drawbacks are a major motivation for the alternative attributes proposed in this paper. For multivariate data, MDTFs are a natural choice, both for the data dimensions themselves as well as derived tensor measures [KKH02].

3. Exploratory visualization

Several researchers underline the value of carrying out visualizations in an exploratory process. Tory and Möller [TM04a] acknowledge that efforts to reduce user input may be counterproductive. Rheingans [Rhe02] points out that the exploration is not only useful as a way to find the best final visualization, it also creates additional understanding during the process. In line with these ideas, the objective for our visualization scheme is to harness the great human ability for advanced and creative analysis, as opposed to replacing it.

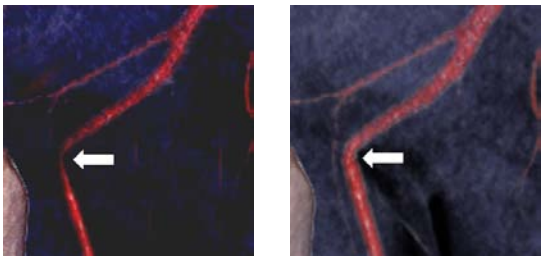

Figure 2: *Static presets can lead to incorrect conclusions, even for calibrated intensities as in this CT angiography. Left: The rendering using the standard TF indicates a stenosis, pointed out by the arrow. Right: Exploring other TF settings clearly shows that there is no stenosis.*

In medical imaging, the problems for automated schemes are particularly challenging since the data sets vary considerably from patient to patient due to the variations in anatomy and examination parameters. The uncalibrated scale of MR images is another complication, hindering preset visualization parameters. CT images have a calibrated scale, but there are slight variations also in this case. One example is given in figure 2, where the standard TF for this CT angiography implied a stenosis. This diagnosis lead to an angioplastic intervention, which turned out to be pointless since no stenosis was found. When the data set was reviewed again by manually adjusting the TF back and forth, i.e. a rudimentary exploratory visualization, it became evident that the stenosis indication was false.

We have identified four requirements that are essential for efficient exploratory visualization schemes:

a) Effective classification features
b) Input in the domain 'language' of the user
c) Simple user interaction
d) Uniform framework for all types of data sets

Existing MDTF design approaches does not fully meet the above requirements: there are many cases when intensity and boundary measures are not sufficient as discriminators (a), gradients and second order derivatives are not intuitive in a non-technical context (b) and complex interaction is often required to construct the MDTFs (c). Explicit classification and segmentation can also be seen as a type of exploratory visualization. They typically provide better discrimination than general TFs (a), but commonly have limitations in interactivity (c) and for more difficult problems they often need to be very specialized, i.e. there is no uniform framework (d). It is clear that exploratory visualization still poses many research challenges.

4. MDTF design concept

The major contributions of this paper is described in this section. We will show that the concept presented in this paper reduces the drawbacks of previous TF approaches and better complies with the requirements of exploratory visualization discussed in section 3. First, novel types of 2D histograms are presented that can replace or act as complement to existing techniques. The following part describes attributes for MDTFs that efficiently increase the classifying capabilities. Then a usage work flow is presented that can accomplish complex visualizations through simple means and finally high-performing simplifications are described.

4.1. Histogram types

Regardless of additional attributes, the most important characteristic for a voxel is always the intensity value. Therefore, all 2D histogram variants in this paper have intensity as the x-axis. Consider the traditional 2D histograms in figure 3. The occurrence of each combination of first and second dimension values is mapped to a color. It is hard to do a quick assessment to find the main characteristics of the data set by comparing voxel clusters in terms of occurrence and value ranges. A 1D histogram provides such an assessment at a glance, thanks to the apparent peak structure. Moreover, peaks in the intensity scale may be difficult to spot altogether in the 2D case since they are smeared across the second dimension. Finally, many data sets have a fairly smooth distribution that makes the 2D histogram cluttered, such as the angiography in figure 3.

Our first suggested 2D histogram type, the *sorted histogram* (fig. 4, left), is based on the idea of keeping the 1D histogram shape, which ensures a direct understanding of the intensity characteristics. The voxels are then sorted according to the value of their second attribute, making high attribute values end up near the top of the histogram curve. Furthermore, the voxels are color-coded according to the second attribute. We use a blue-green-yellow-white color mapping, where white is the maximum value, and black background for all examples in this paper. This paper does not address the issue of finding the perceptually optimal color map. The sorted histogram combines the simplicity of the 1D histogram with the additional information of the traditional 2D histogram.

A limitation of the sorted histogram is that the 1D histogram curve often has very different scale across the intensity value range. A logarithmic scale can help, but it may still be hard to see changes in the distribution of second dimension values, which may be a sign that there is a distinct material hidden in that range. Therefore, we also propose a *Relative sorted histogram* (fig. 4, right). The histogram always fills a rectangular space, and for each intensity (x-axis) value, the sorted relative distribution of second attribute values is shown. An appealing possibility is to display the 1D histogram overlayed on or above the relative sorted histogram to give a frame of reference.

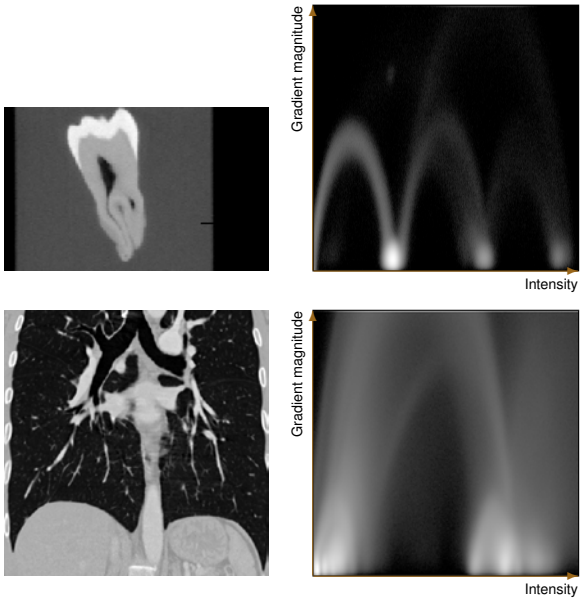

Figure 3: *Limitation of traditional 2D histograms. Top row: The CT tooth from [PBSK00], often used to demonstrate boundary visualizations. Left: A data set slice. Right: The traditional gradient-intensity histogram shows clear arcs representing material boundaries. Bottom row: A CT angiography representing a typical medical data set. Left: A data set slice. Right: The traditional 2D histogram is very cluttered. This comparison demonstrates that traditional 2D histograms have limited usage and that the homogeneous materials and sharp boundaries of the CT tooth is not representative for medical images in general.*

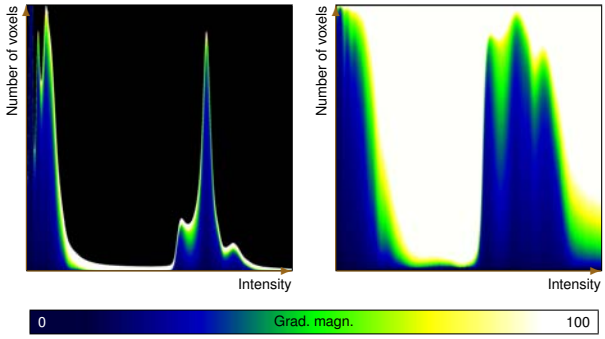

Figure 4: *Proposed 2D histograms of the CT angiography of figure 3. Left:* Sorted histogram*, a 1D intensity histogram is sorted and colored (blue-green-yellow-white) according to a second attribute (here: gradient magnitude). Right:* Relative sorted histogram*, a sorted histogram where the relative distribution of the second attribute is shown.*

4.2. Classifying attributes

Many types of attributes have been used for MDTFs in previous work: gradients, second derivatives, tensors, multivariate data, etc. We will extend this set with a number of attributes derived from intensity values and/or spatial relations. Whereas gradients are good to classify boundaries, they cannot add information on the interior of fairly massive objects such as human organs. Results from recent research [LLY05, LLY] show that *range weight* (w_r) is an effective discriminator for materials with overlapping intensity ranges. The range weight stems from a simple statistical neighborhood analysis and describes the neighborhood footprint in a given partial intensity range Φ:

$$w_r(\Phi, N) = \frac{|N \cap V_\Phi|}{|N|}, \tag{1}$$

where N is an arbitrary voxel neighborhood, V_Φ is the set of voxels within range Φ and $|V|$ is the cardinality of a set V. Range weights can act as proxies for material characteristics that are readily available from domain knowledge: homogeneity, size and shape of materials, as well as proximity to other materials.

Another type of attribute that combines intensity values with spatial relations is *local variance* (σ_n^2), i.e. the variance in the neighborhood of the voxel:

$$\sigma_n^2(N) = \frac{1}{|N|} \sum_{v \in N} \left(I(v)^2 - \left(\sum_{v \in N} \frac{I(v)}{|N|} \right)^2 \right) \tag{2}$$

where $I(v)$ is the value of voxel v. Minor materials are often invisible in the intensity histogram since the background distribution completely covers them. The spatial coherence level, however, may clearly distinguish them, a fact that is exploited in the α-histogram enhancement [LYL*06]. Thus, tissues of interest can be defined by low variance. The opposite may also be true, thin tissues like skin have higher local variance than other elements of similar intensity.

Finally, a natural type of diversifying information is the spatial location of materials. This has typically not been seen as a part of TF models, whereas it is essential for many segmentation schemes, for instance when users set seed points. By incorporating geometric measures in our MDTF concept, the power of these criteria can be utilized in the same way as any other attribute. We use a weighted spatial distance ρ:

$$\rho(\mathbf{x}) = \left(\sum_{i=1}^{3} \left(k_i (x_i - c_i) \right)^2 \right)^{1/2} \tag{3}$$

where $\mathbf{x} = (x_1, x_2, x_3)$ is the voxel position. The reference point (c_1, c_2, c_3) is typically defined by the user and (k_1, k_2, k_3) are optional dimension-specific weighting factors. These measures can easily be turned into static geometric models connected to data set types, e.g. body parts in medical imaging.

4.3. Work flow for MDTF design

For many visualization tasks the optimal rendering can only be achieved by complex criteria in several attribute dimensions, i.e. by an advanced MDTF. Attempts to directly interact with all the dimensions at once is far beyond the capabilities of most users. We propose a work flow where the user works with a sequence of 2D histograms, studying one additional attribute at a time. The MDTF design process is then a matter of switching between second attributes while keeping the frame of reference given by the intensity x-axis. Conclusions made during the process will guide the choice of upcoming attributes to study, resulting in a true exploration of the data. The sorted histograms are particularly suitable for this work flow, since their shape does not change when changing second attribute. Materials are defined by direct range selections (fig. 5) and the process can be summarized as:

1. Define a second attribute of the 2D histogram and select a suitable histogram type.
2. Refine the MDTF by selecting an area in the histogram, creating a material definition criterion
3. If needed, conclude which attribute to study next and restart from step 1.

The area selection in the histogram could be performed with one click to set the range center and mouse movements to set the range size in the two dimensions. As the user switches the second attribute, the voxel selection will have a new distribution for the y-axis and the user can refine the selection (fig. 5). The selected set of voxels are clearly marked in the histogram, as well as the boundary of the criterion in the current dimensions. The color and opacity for the material would typically be set in a separate control. Our approach can be generalized into a range selection function $\Theta(\mathbf{x})$ (eq. 4) defined as a product of threshold functions $\theta_i(s_i(\mathbf{x}))$ with value range $[0.0, 1.0]$, typically consisting of trapezoids and ramps. $s_i(\mathbf{x})$ is the value of variate i at position $\mathbf{x}$.

$$\Theta(\mathbf{x}) = \prod_i \theta_i(s_i(\mathbf{x})) \tag{4}$$

4.4. Simplifications for high performance

A prerequisite of exploratory visualization is that the needed second attributes are not fully known in advance. Most attributes must thus be calculated dynamically. Histogram interaction does not have as high demands on performance as rendering interaction does. Nevertheless, many of the above operations are so time-consuming that they may cause bottlenecks in the work flow. To achieve reasonably accurate approximations very fast, we derive meta-data in form of simplified histograms for non-overlapping cubical block regions in the volume. We employ the straight-forward simplification scheme in [LLYM04] to represent histograms as 12 piece-wise constant segments.

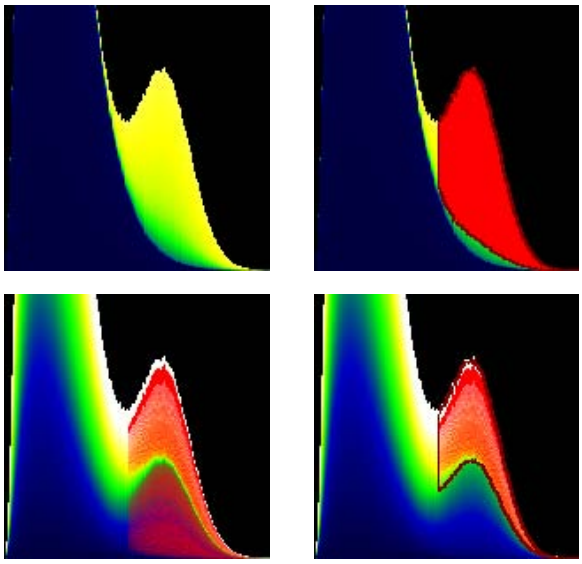

Figure 5: *Transfer Function design through voxel selection in the histogram demonstrated by a synthetic data set. The selected voxels are shown in red (shaded), the criterion in the currently displayed dimensions is shown by dark red curves. Top left: Sorted histogram with a range weight as second attribute. Top right: The user sets a criterion, selecting voxels in an intensity and a range weight interval. Bottom left: The user switches to another second attribute, a spatial distance to a reference point. The selected voxels form two clusters in this dimension. Bottom right: The user sets a criterion selecting the top cluster, i.e. voxels far from the reference point.*

Using the simplified histograms, range weight and local variance attributes can be calculated at block level. The full 2D histograms and the set of selected voxels within them can then efficiently be computed. One possibility is to derive individual attribute values for each voxel as a linear interpolation of values of the nearest blocks. Another solution is to let all voxels in a block be approximated by the attribute value of the corresponding block and assign voxel intensities according to the simplified histogram. Such a solution is shown in figure 6.

Another approach for calculating range weights and local variance with intermediate quality and performance is to replace the full spherical neighborhood operators by 3D cross neighborhoods instead, see [LLY] for details.

5. Results

This section will present histogram displays and resulting renderings that exemplify some benefits of sorted histograms. The DVR images have been created by a single-pass, GPU-based raycaster [SSKE05] working on multivari-

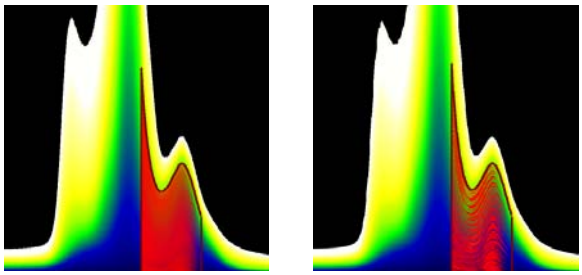

Figure 6: *Histogram approximation. Left: Part of a sorted histogram of the angiography in figure 4 with selected voxel set (red/shaded). Right: An approximation where both the sorted histogram and the voxel selection are estimated from block-level meta data.*

ate data represented as separate volumes. The resulting color $\mathbf{c}$ of each sample is given by the range selection functions $\Theta_m(\mathbf{x})$ (eq. 4) and transfer functions $\tau_m(s_0)$ defined for each material m, where s_0 is the intensity sample:

$$\mathbf{c}(\mathbf{x}) = \sum_m \tau_m(s_0) \cdot \Theta_m(\mathbf{x}) \tag{5}$$

In the examples below the materials have non-overlapping ranges, i.e. only one Θ_m function is non-zero at each position. Within overlapping ranges, $\mathbf{c}$ should instead be set as the average of the non-transparent materials for the sample.

In order to demonstrate the work flow of section 4.3 we describe a potential usage scenario for the MR bile duct examination in figure 7 and color plate figure C1. An exploratory visualization session is started by displaying an α-histogram enhancement of the data set (fig. 7a). An unexpected secondary peak appears. To investigate this further, a sorted histogram is created with the range weight (spherical neighborhood, radius 3.0 voxels) for the peak interval as second attribute (fig. 7b). The top part of the histogram peak is then selected in order to visualize the corresponding voxels. This makes a liver tumor appear, but also a significant amount of non-relevant tissues such as the spleen (top right) and other disturbing fragments (fig. 7d). Therefore, the second attribute is changed into a spatial radius measure through a mouse click at the center of the liver tumor. Then the tumor region can be easily selected in the sorted histogram (fig. 7c), making the tumor clearly rendered without cluttering (fig. 7e).

An important part of forensic visualizations is the study of metal fragments since they can indicate the path of bullets and if the bullet was deflected before entering the body. Results from a virtual autopsy, usually a DVR visualization of a CT scan of the human cadaver, is crucial to the criminal investigation. A problem is that minor metal fragments can be overlooked since their location may be unexpected. Using the proposed techniques in form of a range weight attribute (spherical neighborhood, radius 6.0 voxels) makes it possible to highlight not only the fragments, but also a neighborhood of the fragments as in color plate figure C2, making the visual localization much more simple.

Table 1: *Error vs. performance of simplified attributes, top: range weight, bottom: local variance. Neighborhoods – Exact measures: sphere of radius* $5.0 = 514$ *voxels, 3D cross: radius* $5 = 30$ *voxels, block:* $8^3 = 512$ *voxels. "Block" refers to calculation at block level, "Block & interp." further include deriving voxel-specific values. CT tooth: 256x256x160 voxels (last slice ignored to make even blocks), MR bile: 256x256x112 voxels. Times in seconds, SNR in dB.*

Range weight	CT tooth		MR bile	
	Time	SNR	Time	SNR
Exact	97.3	∞	65.3	∞
3D cross	1.83	18.3	1.39	18.0
Block	0.007	-	0.005	-
Block & interp.	0.49	12.9	0.37	15.1

Local variance	CT tooth		MR bile	
	Time	SNR	Time	SNR
Exact	98.6	∞	65.4	∞
3D cross	2.40	25.6	1.69	19.8
Block	0.007	-	0.006	-
Block & interp.	0.49	18.2	0.37	16.5

An annoying problem of CT scans is that metal regions cause severe streaking artefacts such as those originating from the dental work in figure 8. One effect is that a rendering of the skin will be very incorrect around these metallic regions. The proposed framework provides a possibility to separate these artefacts from real skin by studying the variance: since real skin is close to both air and other soft tissue it has higher variance than the slowly varying surrounding of streaking metal artefacts. Selecting high-variance voxels (spherical neighborhood, radius 2.0 voxels) effectively removes the artefacts, as seen in figure 8. Other 'false skin' voxels such as the bed in the background are also removed.

The approximations of range weight and local variance based on simplified block histograms (section 4.4) have been evaluated, see table 1. The calculation times are dramatically reduced and the introduced error in the attribute volume is moderate. A natural approach is to use the approximations during histogram interaction and retrieve the exact values when interaction stops. Figure 6 shows that the error due to these approximations in a sorted histogram is minor.

6. Conclusions

We have presented a design concept for MDTF design, introducing sorted histograms as a convenient way of defining a material through criteria in multiple dimensions. Even in the case when the color mapping of the second attribute does not reveal new information, the sorting enables efficient material definitions through direct selection in the sorted histogram.

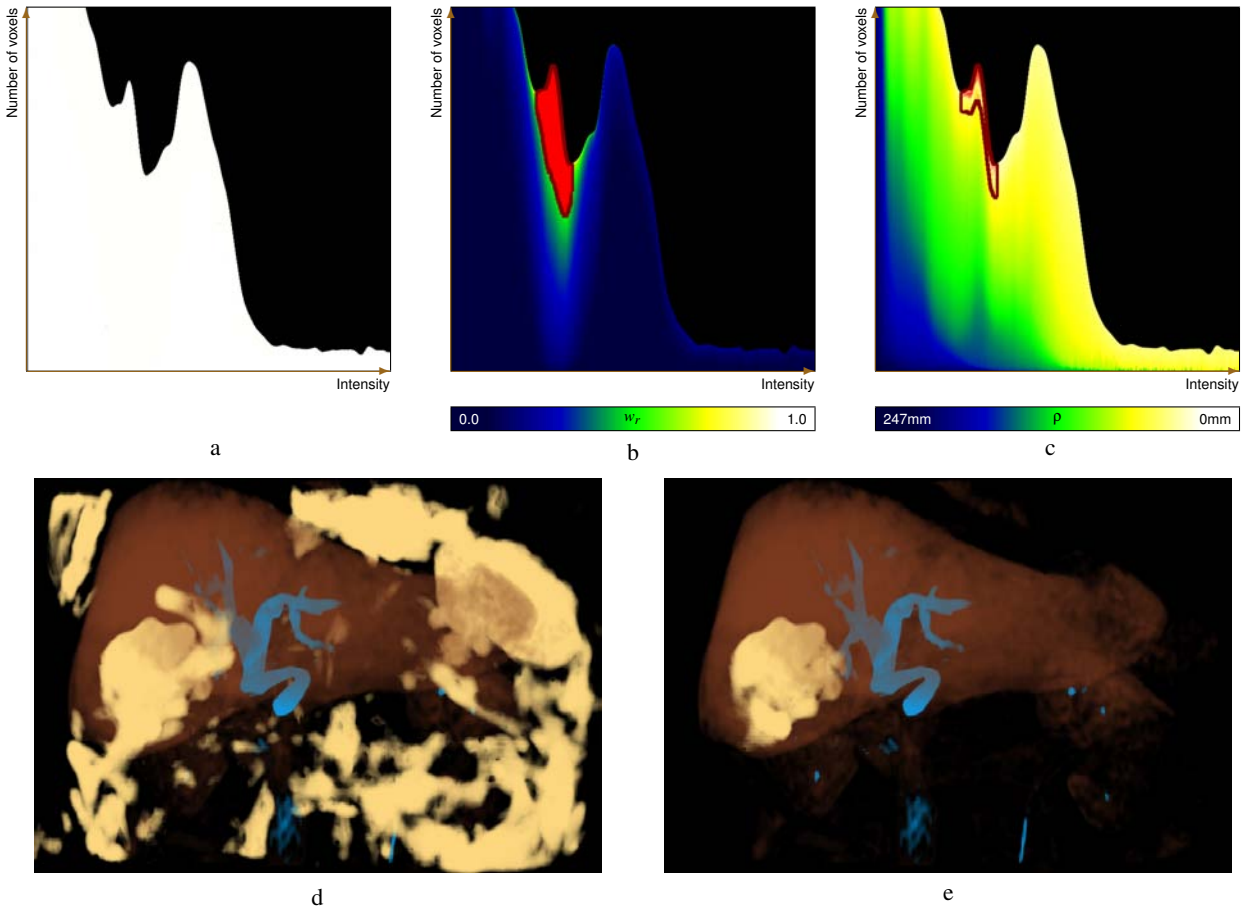

Figure 7: *Work flow of creating a MDTF that highlights the liver tumor, see text for details. The histograms do not show material definitions for liver (large triangular object) or bile duct ('tree' at the liver center). a) An α-histogram reveals a minor peak. b) A sorted histogram highlighting coherent tissue in the range of the peak is the first classification step. c) Non-relevant tissue fragments are removed through another sorted histogram showing spatial distance from the tumor center. d) Rendering using the coherence criterion only. e) Rendering with both criteria, a clear view of the tumor (low left part of the liver).*

Although preliminary user reactions are positive, we need to conduct a thorough user study in order to draw reliable conclusions about the benefits and limitations of sorted histograms as a TF construction tool.

The range weight and local variance attributes proposed in this paper have been put to successful use as additional variates of the data set. They have proven to accomplish visualization objectives that were not possible with previous 1D TF or MDTF approaches. The range weight is especially useful since it can be adapted to the conclusions drawn during the exploration. We have also shown that the measures can be efficiently calculated using block-level meta data. A limitation is that it is impractical to store meta data for all block sizes, making the neighborhood-based measures less flexible. Furthermore, we have demonstrated that geometric criteria can be treated as additional attributes, enabling a uniform handling of all user input to the MDTF.

Acknowledgements

This work has been conducted at the Center for Medical Image Science and Visualization (CMIV) at Linköping University, Sweden. CMIV is acknowledged for provision of financial support and access to leading edge research infrastructure. The work was funded by the Swedish Research Council, grants 621-2003-6582 and 621-2001-2778, and the Swedish Foundation for Strategic Research, grant A3 02:116.

References

[HHKP96] HE T., HONG L., KAUFMAN A., PFISTER H.: Generation of transfer functions with stochastic search techniques. In *Proceedings IEEE Visualization 1996* (1996), pp. 227–234.

[HKG00] HLADÚVKA J., KÖNIG A. H., GRÖLLER E. M.: Curvature-based transfer functions for direct volume rendering. In *Proceedings Spring Conference Computer Graphics 2000* (2000), vol. 16, pp. 58–65.

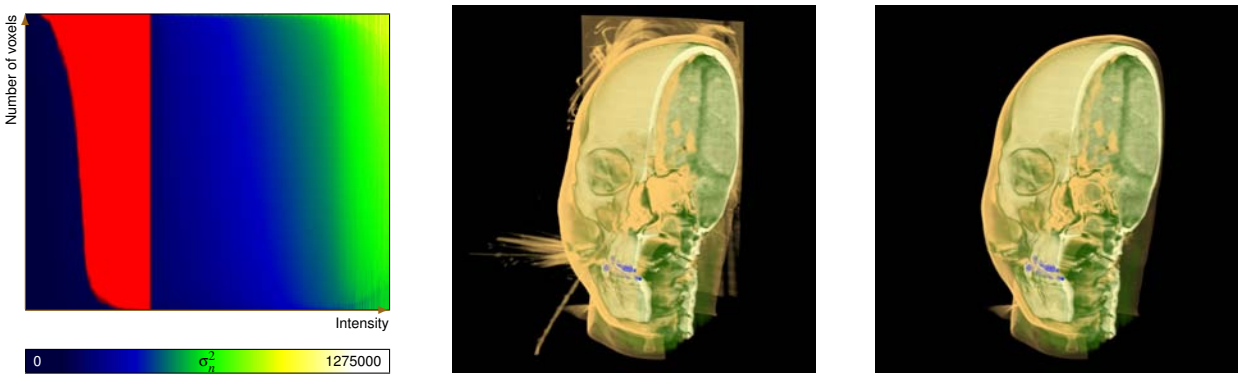

Figure 8: *Removing false skin, e.g. artefacts from metal in the teeth, in the Chapel Hill CT Head. By selectively showing voxels with high variance the true skin voxels are shown but not the artefacts from metallic regions or the bed surface in the background. a) A relative sorted histogram showing local variance where high variance voxels are selected (red) in the skin value range. b) Rendering with a 1D TF where the streak artefacts from the tooth fillings falsely appear as skin. c) Rendering with the 2D TF based on variance.*

[KD98] KINDLMANN G., DURKIN J. W.: Semi-automatic generation of transfer functions for direct volume rendering. In *Proceedings IEEE Symposium on Volume Visualization* (1998), pp. 79–86.

[KG01] KÖNIG A. H., GRÖLLER E. M.: Mastering transfer function specification by using VolumePro technology. In *Proceedings Spring Conference Computer Graphics 2001* (2001), vol. 17, pp. 279–286.

[KKH02] KNISS J., KINDLMANN G., HANSEN C.: Multidimensional transfer functions for interactive volume rendering. *IEEE Transactions on Visualization and Computer Graphics 8* (2002), 270–285.

[KWTM03] KINDLMANN G., WHITAKER R., TASDIZEN T., MÖLLER T.: Curvature-based transfer functions for direct volume rendering: Methods and applications. In *Proceedings IEEE Visualization 2003* (2003), pp. 513–520.

[Lev88] LEVOY M.: Display of surfaces from volume data. *IEEE Computer Graphics and Applications 8*, 5 (1988), 29–37.

[LLY] LUNDSTRÖM C., LJUNG P., YNNERMAN A.: Local histograms for design of Transfer Functions in Direct Volume Rendering. *IEEE Transactions on Visualization and Computer Graphics*. Accepted for publication.

[LLY05] LUNDSTRÖM C., LJUNG P., YNNERMAN A.: Extending and simplifying Transfer Function design in medical Volume Rendering using local histograms. In *Proceedings IEEE/EuroGraphics Symposium on Visualization* (2005), pp. 263–270.

[LLYM04] LJUNG P., LUNDSTRÖM C., YNNERMAN A., MUSETH K.: Transfer function based adaptive decompression for volume rendering of large medical data sets. In *Proceedings IEEE Volume Visualization and Graphics Symposium* (2004), pp. 25–32.

[LM04] LUM E. B., MA K.-L.: Lighting transfer functions using gradient aligned sampling. In *Proceedings IEEE Visualization 2004* (2004), pp. 289–296.

[LYL*06] LUNDSTRÖM C., YNNERMAN A., LJUNG P., PERSSON A., KNUTSSON H.: The α-histogram: Using spatial coherence to enhance histograms and Transfer Function design. In *Proceedings IEEE/EuroGraphics Symposium on Visualization* (2006), pp. 227–234.

[MAB*97] MARKS J., ANDALMAN B., BEARDSLEY P., FREEMAN W., GIBSON S., HODGINS J., KANG T., MIRTICH B., PFISTER H., RUML W., RYALL K., SEIMS J., SHIEBER S.: Design galleries: A general approach to setting parameters for computer graphics and animation. In *Proceedings SIGGRAPH 1997* (1997), pp. 389–400.

[PBSK00] PFISTER H., BAJAJ C., SCHROEDER W., KINDLMANN G.: The transfer function bake-off. In *Proceedings IEEE Visualization 2000* (2000), pp. 523–526.

[Rhe02] RHEINGANS P.: Are we there yet? Exploring with dynamic visualization. *IEEE Computer Graphics and Applications 22* (2002), 6–10.

[SSKE05] STEGMAIER S., STRENGERT M., KLEIN T., ERTL T.: A simple and flexible volume rendering framework for graphics-hardware–based raycasting. In *Eurographics/IEEE Volume Graphics Symposium* (2005), Eurographics.

[ŠVSG06] ŠEREDA P., VILANOVA BARTROLÍ A., SERLIE I. W. O., GERRITSEN F. A.: Visualization of boundaries in volumetric data sets using LH histograms. *IEEE Transactions on Visualization and Computer Graphics 12*, 2 (2006), 208–218.

[TLM03] TZENG F.-Y., LUM E. B., MA K.-L.: A novel interface for higher-dimensional classification of volume data. In *Proceedings IEEE Visualization 2003* (2003), pp. 505–512.

[TM04a] TORY M., MÖLLER T.: Human factors in visualization research. *IEEE Transactions on Visualization and Computer Graphics 10* (2004), 72–84.

[TM04b] TZENG F.-Y., MA K.-L.: A cluster-space visual interface for arbitrary dimensional classification of volume data. In *Proceedings Eurographics/IEEE TCVG Visualization Symp. (VisSym)* (2004), pp. 17–24.